Real-time edge enhancement of femtosecond time-domain images by use of photorefractive quantum wells

Y. Ding and D. D. Nolte

Department of Physics, Purdue University, 1396 Physics Building, West Lafayette, Indiana 47907-1396

M. R. Melloch and A. M. Weiner

School of Electrical and Computer Engineering, Purdue University, West Lafayette, Indiana 47907

Received March 6, 1997

Dynamic holograms written in a photorefractive multiple quantum well placed inside a Fourier femtosecond pulse shaper convert a space-domain image into the time domain. We demonstrate that edge-enhancement processing of the time-domain image can be performed by controlling hologram-writing intensities. © 1997 Optical Society of America

Time-to-space conversions are important for optical signal processing, optical transmultiplexing, image processing, and temporal pattern generation and recognition. Both time-to-space and space-to-time conversions have been demonstrated,[1–3] and time-domain images have been obtained with fixed Fourier holograms and dynamic liquid-crystal spatial light modulators.[3–5] Processing time-domain images (by analogy with image processing of conventional space-domain images) includes convolution, correlation, matched filtering, edge enhancement, and noise suppression. With spectral holography,[6] operations such as time reversal and matched filtering of optical pulses have been realized.[7,8] Other pulse-shaping approaches such as nonlinear spectral holography and volume reflection holograms may permit more-elaborate processing operations.[9,10] Edge enhancement for time-domain images would be interesting for optical communication and image-processing applications such as header recognition of a coded information packet, feature extraction, and separation of closely neighboring ultrashort pulses. In this Letter we demonstrate image space-to-time conversion and edge enhancement of the converted time-domain images by using femtosecond pulse-shaping techniques and photorefractive multiple quantum wells (MQW's) as holographic media.[11,12] Because the holograms here are dynamic, the conversion and image processing occur in real time, limited only by the material response time, which is typically microseconds.

The experimental setup is shown in Fig. 1 and consists of a femtosecond pulse-shaping apparatus with a photorefractive MQW placed in the Fourier plane performing as a holographic medium.[12] Except for the hologram-writing geometry, the parameters of the pulse shaper are the same as in Ref. 12. The hologram is written in the MQW by two writing beams incident in a vertical plane from a cw diode laser operating at 685 nm with a power of ~7 mW in each beam and a spot size of 1.5 mm × 4 mm. A cylindrical lens (f = 150 mm) is put into one of the writing beams, called the image-carrying beam, to project the Fourier transform of a spatial image (here a single slit with a width of 380 μm) onto the MQW. The image Fourier plane is 22 deg off the Fourier plane of the pulse shaper, for technical simplicity. Because of the long focal length of the Fourier lens, this difference in location of the Fourier planes had no major influence on our results. Neutral-density filters are used to adjust the beam intensities. The femtosecond source is a mode-locked Ti:sapphire laser with a nominal pulse width of 100 fs and a central wavelength of 835 nm. The femtosecond probe beam with a power of 2.6 mW and a diameter of 1.8 mm is incident upon the first grating of the pulse shaper (Fig. 1) and spectrally dispersed. The separated frequency components are diffracted from the hologram in the MQW at the Fourier plane. The diffracted optical components are then recombined by the second cylindrical lens and the second grating, forming the femtosecond output carrying the information from the hologram. The spectrum of the femtosecond output is measured by a spectrometer with a CCD array, and the temporal shape of the pulse is measured by electric-field cross correlation[13] with an unshaped approximately transform-limited reference pulse. The photorefractive medium is a $GaAs/Al_{0.3}Ga_{0.7}As$ MQW. A dc voltage of 700 V is applied with the direction parallel to the MQW layers (transverse-field geometry[11]),

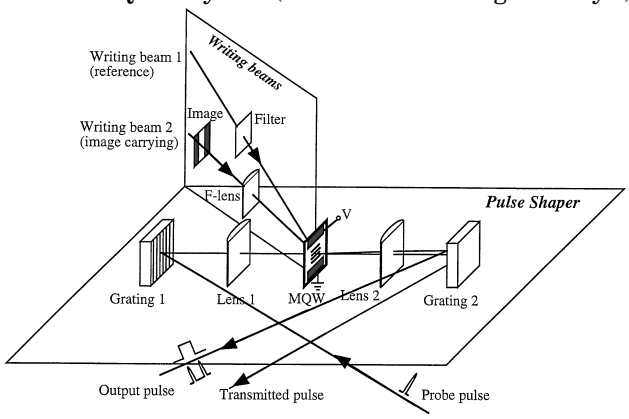

Fig. 1. Experimental setup for space-to-time conversion and edge enhancement of femtosecond time-domain images by use of dynamic holograms written in a photorefractive MQW: F-lens, Fourier lens; V, applied voltage.

0146-9592/97/141101-03$10.00/0

giving an output diffraction efficiency of the order of 0.1%. Because of the 1-mm electrode gap on the MQW, the spatial profile of the output is ellipsoidal, with a size of 1 mm × 2 mm. Although electroabsorption and electrorefraction are strongly dispersive, it was shown that the diffraction from a transverse-field geometry MQW is not distorted as a result of the Kramers–Kronig causality.[12]

Using the experimental setup in Fig. 1, we can convert an image from the space domain into the time domain. We can also perform edge enhancement on the converted time-domain image by choosing an appropriate hologram-writing intensity ratio. The interference pattern of two coherent writing beams has a modulation depth of

$$m(x) = \frac{2E_1E_2(x)}{|E_1|^2 + |E_2(x)|^2} = \frac{2[I_1I_2(x)]^{1/2}}{I_1 + I_2(x)}, \qquad (1)$$

with the field amplitude E_1 (intensity I_1) of the reference writing beam (spatially homogenous) and those of the image-carrying beam $E_2(x)$ $[I_2(x)]$. We see from Eq. (1) that m depends only on the intensity ratio of the two beams I_2/I_1 and has the maximum value of unity when $I_2 = I_1$. The hologram written in the MQW is proportional to m as long as m is small. As m approaches unity, the amplitude of the photorefractive grating, and therefore the diffracted electric-field amplitude as well, is sublinear with m.[14]

In holographic recording, the hologram pattern is a faithful replica of the original electric-field distribution only if the intensity of the image-carrying beam is much less than the intensity of the reference beam and the material response is linear in intensity. In this case $[I_1 \gg I_2(x)]$ we get, from Eq. (1), $m(x) \sim E_2(x)$; i.e., the hologram has the same distribution as the image-carrying beam $E_2(x)$. In the opposite case, when the reference beam is weaker than the image-carrying beam at certain positions in the interference pattern, the corresponding $m(x)$ varies as $E_1/|E_2|$, indicating a grating amplitude (as well as the diffraction amplitude) at these positions, which decrease with increasing $|E_2|$. As a result, the hologram amplitude saturates for positions where $I_2(x) \geq I_1$. Such saturations can serve to enhance high-frequency optical frequency components at the expense of a strong peak at the center frequency, yielding a type of high-pass filtering that can lead to edge enhancement in the reconstructed images. Such effects have been demonstrated in the space domain[15] and used to detect dust and other small defects in photolithographic masks.[16]

In our setup in Fig. 1, if the hologram in the MQW is a faithful Fourier transform of a given space-domain image the diffracted temporal signal should take on the same temporal shape as the input space-domain image. This is the case of space-to-time conversion. For the hologram in the MQW to be a faithful Fourier transform of the space-domain image the reference-beam intensity must be higher than the most intense spot of the Fourier transform of the image-carrying beam. Otherwise, the brightest spots in the Fourier plane will be suppressed, which, for images that have a low-pass character (such as the square in our experiments), would lead to edge enhancement.

We performed experiments for both intensity ratio cases. In the first case the reference-beam intensity is higher than the most intense spot of the Fourier transform of the image. The far-field intensity distribution of a single-slit diffraction takes the form of a squared sinc function when the coordinate in the Fourier plane x is much smaller than the Fourier lens focal length f:

$$F = \sin^2\left(\frac{2\pi Dx}{\lambda f}\right)\Big/\left(\frac{2\pi Dx}{\lambda f}\right)^2, \qquad (2)$$

with the slit width $2D = 380$ μm and the writing wavelength $\lambda = 685$ nm. From Eq. (2), the FWHM of the main maximum of the distribution is ~250 μm. The intensity of this maximum is not more than twice as large as that of the beam in front of the lens. Neutral-density filters are used to reduce the image-carrying beam intensity by an order of magnitude. At the Fourier plane in the pulse shaper the projection of the intensity distribution in Eq. (2) interferes with the reference writing beam and induces a hologram in the MQW with the same distribution. The diffracted spectrum from the hologram takes the same distribution as shown in Fig. 2(a). For comparison, a theoretical curve obtained with Eqs. (1) and (2) is also given, where the spectral dispersion of the pulse shaper of 0.36 mm/nm and the MQW spectral response with a intensity FWHM of 4.2 nm were used. The spectrum agrees well with the simple theory. The finite spectral resolution of the system and the angle between the image Fourier plane and the Fourier plane in the pulse shaper cause the minima of the intensity distribution in the experimental data not to drop to zero as in the theory.

For the edge-enhancement experiment the intensity of the reference beam is reduced by 2 orders of magnitude relative to that of the image-carrying beam. As a result, the interference of the two writing beams (the hologram) cuts off the primary maximum in the image-carrying beam and extracts the higher-spatial-frequency components of the slit diffraction (sidelobes with lower intensities) that describe edges. The diffracted spectrum from such a hologram is shown in Fig. 2(b).

The temporal shapes of the diffracted femtosecond outputs, which are the Fourier transforms of the electric field spectra corresponding to the power spectra in Fig. 2, are shown in Fig. 3. The time-domain image in Fig. 3(a) corresponds to the input space-domain image, which is a slit or a square-wave packet. Several factors in the diffraction process prevent the second-stage Fourier transform (Fourier transform from the frequency domain to the time domain) from transforming all the frequency components to the time domain. The finite spectral bandwidth of the material response, which is determined by the electroabsorption of the excitons in the MQW and has an approximately Gaussian shape, reduces the sharpness of the steps in the square-wave packet. The ratio of the spectrally dispersed femtosecond probe beam intensity to the writing intensity can influence the modulation in Eq. (1), resulting in some modulations including small sidelobes in the reconstructed image. Any asymmetry in the spectra

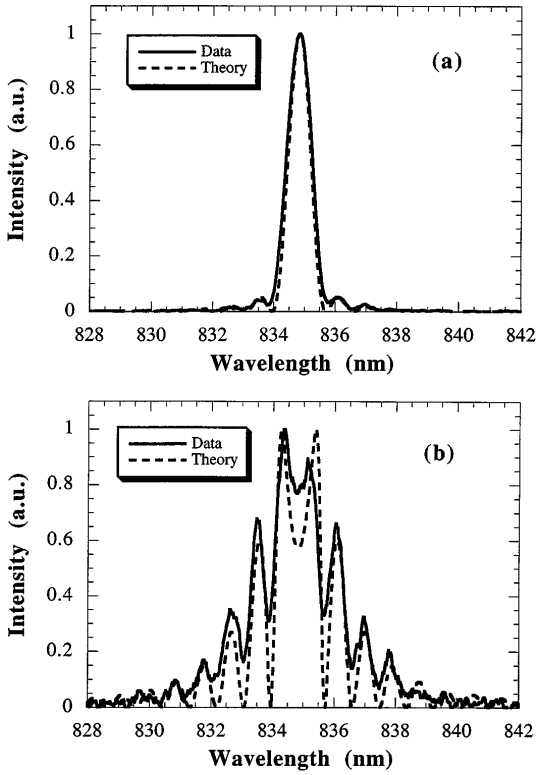

Fig. 2. Spectra of the diffracted temporal images when the reference beam's intensity is (a) higher and (b) lower than the image-carrying beam's intensity. The theoretical calculations for (a) $I_1/I_{2\mathrm{Max}} = 10$ and (b) $I_1/I_{2\mathrm{Max}} = 0.01$ are also shown.

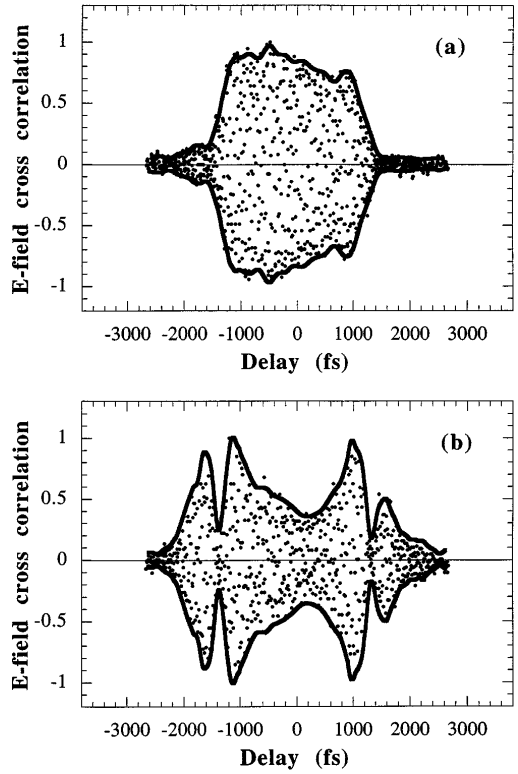

Fig. 3. Electric-field cross-correlation data and the extracted envelopes of the diffracted temporal images when the reference beam's intensity is (a) higher and (b) lower than the image-carrying beam's intensity, showing (a) space-to-time conversion and (b) edge enhancement.

owing to the misalignment of the image Fourier lens will also introduce modulations in the time-domain image. Special care is taken in our experiments to minimize the influence of these factors, and we get an approximate square-wave packet. Notice that Fig. 3(a) contains the electric-field cross-correlation data. The sidelobes would appear much smaller if the intensity rather than the field amplitude were plotted. Figure 3(b) shows the diffracted output in the case when the reference writing beam is weaker, corresponding to the spectrum in Fig. 2(b). By comparing Figs. 3(b) and 3(a), we see that the edge features in the time-domain image in Fig. 3(a) are strongly enhanced. The side wings in Fig. 3(b) are also expected from the theoretical Fourier transform of Eq. (1) with Eq. (2). The idea of realizing processing operations such as edge enhancement by controlling the hologram-writing intensities can also be used in the pure time domain (no space-to-time conversion needed), in which the writing beams sent into the pulse shaper are time-domain image-carrying beams (like coded pulse packets in previous spectral holography experiments[7,8]) instead of the cw laser beams used in this experiment.

The authors gratefully acknowledge support from the U.S. Department of Defense Focused Research Initiative through U.S. Air Force Office of Scientific Research grant F49620-95-1-0533, National Science Foundation grant 9414800-ECS, and Rome Labs grant F30602-96-2-0114.

References

1. M. C. Nuss, M. Li, T. H. Chiu, A. M. Weiner, and A. Partovi, Opt. Lett. **19,** 664 (1994).
2. K. Ema, Japn. J. Appl. Phys. **30,** L2046 (1991).
3. M. C. Nuss and R. L. Morisson, Opt. Lett. **20,** 740 (1995).
4. A. M. Weiner, D. E. Leaird, J. S. Patel, and J. R. Wullert, IEEE J. Quantum Electron. **28,** 908 (1992).
5. M. M. Werfers and K. A. Nelson, Opt. Lett. **20,** 1047 (1995).
6. Y. T. Mazurenko, Appl. Phys. B **50,** 101 (1990).
7. A. M. Weiner, D. E. Leaird, D. H. Reitze, and E. G. Paek, IEEE J. Quantum Electron. **28,** 2251 (1992).
8. A. M. Weiner, D. E. Leaird, D. H. Reitze, and E. G. Paek, Opt. Lett. **17,** 224 (1992).
9. A. M. Weiner and D. E. Leaird, Opt. Lett. **19,** 123 (1994).
10. K. B. Hill and D. J. Brady, Opt. Lett. **18,** 1739 (1993).
11. D. D. Nolte and M. R. Melloch, in *Photorefractive Effects and Materials*, D. D. Nolte, ed. (Kluwer, Dordrecht, The Netherlands, 1995).
12. Y. Ding, R. M. Brubaker, D. D. Nolte, M. R. Melloch, and A. M. Weiner, Opt. Lett. **22,** 718 (1997).
13. K. G. Purchase, D. J. Brady, and K. Wagner, Opt. Lett. **18,** 2129 (1993).
14. Ph. Refrégiér, L. Solymar, H. Rajbenbach, and J. P. Huignard, J. Appl. Phys. **58,** 45 (1985).
15. J. P. Huignard and J. P. Herriau, Appl. Opt. **17,** 2671 (1978).
16. E. Ochoa, J. W. Goodman, and L. Hesselink, Opt. Lett. **10,** 430 (1985).